Analysis of Elastic-Plastic Behavior of Fiber Metal Laminates Subjected to In-Plane Tensile Loading

H. Esfandiar*
Department of Mechanical Engineering,
Firozkouh Branch, Islamic Azad University, Firozkouh, Iran
E-mail: habib_esfandiar_2006@yahoo.com
*Corresponding author

S. Daneshmand
Department of Mechanical Engineering,
Majlesi Branch, Islamic Azad University, Isfahan, Iran
E-mail: Saeed_daneshmand@yahoo.com

M. Mondali
Department of Mechanical and Aerospace Engineering,
Science and Research Branch, Islamic Azad University, Tehran, Iran
E-mail: mondali@srbiau.ac.ir

Abstract: Fiber metal laminates are hybrid laminates consisting of thin alternating bonded layers of aluminum and fiber/epoxy. ARALL (Aramid aluminum laminate) and GALARE (glass fiber reinforced aluminum laminate) are specific kinds of fiber metal laminates that consist of thin aluminum sheets along with Kevlar/Epoxy and Glass/Epoxy composite layers, respectively. In this study, nonlinear tensile behavior of GLARE fiber metal laminates under in-plane loading conditions has been investigated. Due to the elastic-plastic behavior of aluminum layers, elastic analyses are not enough to accurately predict the tensile response. Thus, it is necessary to consider and explain the inelastic deformation behavior of GLARE laminates after yielding of aluminum alloy layers. Two appropriate analytical approaches, the orthotropic plasticity and modified classical laminated plate theories, have been used to predict the stress-strain response and deformation behavior of GLARE laminates. An acceptable agreement was observed between the two models. Results show that the GLARE behavior is almost bilinear under tensile loading condition and the tensile strength of unidirectional GLARE laminates are substantially stronger than aluminum alloys in the longitudinal direction.

Biographical notes: H. Esfandiar and **S. Daneshmand** are PhD students of Mechanical Engineering at Science and Research Branch, IAU, Tehran, Iran. **M. Mondali** received his PhD in Mechanical Engineering from Sharif University of Technology. He is currently Assistant Professor at Department of Mechanical and Aerospace Engineering, Science and Research Branch, IAU, Tehran, Iran.

1 INTRODUCTION

Fiber-Metal Laminates (FMLs) are hybrid laminates built up from thin aluminum alloy sheets bonded into laminates by intermediate thin fiber/epoxy layers. Their behavior is a mixture of metals and composites, they have high damage tolerance properties, and were primarily developed for aerospace applications where good fatigue properties and high strength are necessary [1]. Design and development of advanced composite materials have always attracted great interests to improve mechanical properties and their performance in advanced structures such as aircraft structures [2, 3]. Recent advances using composites in modern aircraft construction were reviewed and carbon fiber composites were particularly argued in terms of design, manufacture and applications [4]. Fiber Metal Laminates were developed at Delft University of Technology in The Netherlands by L. B. Vogelesang [5]. The Basic idea for the development of fiber metal laminates was to develop a material with a high crack growth resistance for fatigue prone areas of modern civil aircraft [5, 6]. It is reported that FMLs originated at Fokker/TU Delft in the Netherlands about 1970s, and since then have undergone extensive development [7, 8]. Aluminum alloys are most commonly used in FMLs as metal, and the fibers can be Kevlar or glass [9]. The first commercial product of FMLs under the trade name ARALL, including Kevlar/Aramid as fibers, was launched by ALCOA in 1982 for aircraft wing application. A patent on GLARE was filed in October 1987 by AKZO that was composed of aluminum alloy sheets and unidirectional or biaxial reinforced high strength glass fiber/epoxy composite layers [10, 11]. The main reason for switching to glass fibers is that aramid fibers failed at some loading conditions. But, fiber failure is unacceptable for the excellent fatigue resistance of FML. The glass fiber ply in GLARE does not have the disadvantage of failing fibers, and therefore GLARE became the most important variant for FML [12]. Recently, GLARE laminate was selected for the upper fuselage skin structures of Airbus A380. This is the first structural application of GLARE laminate in a commercial air-line. Each A380 will have about 380 m of GLARE. The GLARE laminates are also applied in the leading edges of the vertical and horizontal tail planes of the A380 [9]. Limiting attention to the mechanical properties and in particular to the tensile response, it has been shown [13, 14] that the stress-strain curve of an FML is highly nonlinear, mainly reflecting the plasticity of the metal sheets. It is well documented that FMLs combine the durability of metals with the impressive fatigue and fracture properties of fiber-reinforced composite materials [15, 16]. Krishnakumar [15] showed that the tensile strength of many fiber-metal laminates is superior to that of traditional aerospace-grade aluminum alloys. Wu et.al investigated the in-plane mechanical properties of GLARE 4 with 2/1, 3/2 and 5/4 lay-up. The mechanical properties of GLARE4 were also predicted using the metal volume fraction approach based on a rule of mixtures [17]. Nahas presented several models for nonlinear deformation of FMLs [18]. Since, GLAREs consist of aluminum layers and aluminum has nonlinear behavior, therefore elastic analysis is not sufficient hence a model for exact prediction of nonlinear tensile response must be presented. To achieve such a model, glass/epoxy composite should be modeled as an orthotropic linearly elastic solid and aluminum is assumed as an elasto-plastic solid. In the present research, the nonlinear tensile response of GLARE laminate is investigated under static tensile loading condition. Two approaches as orthotropic plasticity and modified laminated plate theories are used to predict the stress-strain response and deformation behavior of GLARE laminate. In the orthotropic plasticity model, a three parameter plastic potential function is used. In the second theory, the composite layers and aluminum sheets are assumed to be linearly elastic and orthotropic elastic–plastic solids, respectively.

2 CASE STUDY

Several GLARE grades are commercially available (see Table (1)). Every grade can be built up in many different thicknesses, e.g., the lay-up of a GLARE 5 variant with a so-called '2/1 lay-up' as shown in Fig. 1 is:

2024-T3 aluminum/ $0°$ glass fiber/ $90°$ glass fiber/ $90°$ glass fiber/ $0°$ glass fiber/ 2024-T3 aluminum in which the 0 direction is the longitudinal direction (i.e., the rolling direction) of the aluminum layers. The most important properties of GLARE are as follows [1]:

- It has the fatigue behavior of an aluminum alloy, although the fiber layers of the material improve this behavior significantly.
- GLARE is affected by hot-wet ageing under accelerated conditions, as with composites. However, moisture absorption (through the milled edges only) and property reductions are less compared to glass composites due to the large amount of unaffected aluminum in the material.

- The specific weight of GLARE is approximately 10% lower than that of aluminum.
- GLARE is formable to many single and double curved shapes (Fig. 6).
- GLARE tensile strength is significantly higher than 1.5 $\times$ yield stress.
- GLARE blunt notch strength is often one of the governing design values.
- GLARE can be machined using similar tools (hard metal steel) and procedures as for aluminum alloys.
- GLARE can be repaired using aluminum type repair configurations and procedures.

In this paper, the nonlinear tensile response of selected cross-plied GLARE 4 and GLARE 5 laminates is investigated under static tensile loading conditions. GLARE 4-3/2 consists of three layers of 2024-T3 aluminum alloy sheets and two layers of 70/30 glass prepreg with 67% of fibers in the 0° direction and 33% fiber in the 90° direction. GLARE 5-2/1 laminates consist of two layers of 2024-T3 aluminum alloy sheets with one layer of 50/50glass prepreg with 0°/90°/90°/0°fiber orientation.

The 2024–T3 aluminum alloy and Glass/epoxy are modeled as elasto–plastic and orthotropic linearly elastic solids, respectively. Mechanical properties of aluminum alloy and Glass/epoxy have been presented in table 2.
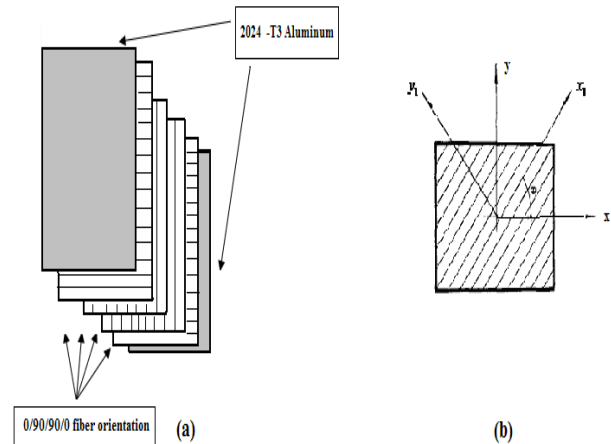
Fig. 1 (a) The schematic view of GLARE 5-2/1 (b) Definitions coordinate for composite

Table 1 Commercially available GLARE grades [1, 9]

GLARE grade	Aluminum Layers		Fiber Layers		Typical Density (g/cm^3)
	Alloy	Thickness per Layers (mm)	Orientation	Thickness per layer (mm)	
GLARE 1	7475-T76	0.3-0.4	Unidirectional	0.25	2.52
GLARE 2	2024-T3	0.2-0.5	Unidirectional	0.25	2.52
GLARE 3	2024-T3	0.2-0.5	$0°/90°$ Cross-ply (50%-50%)	0.25	2.52
GLARE 4	2024-T3	0.2-0.5	$0°/90°/0°$ Cross-ply (67%-33%)	0.375	2.45
GLARE 5	2024-T3	0.2-0.5	$0°/90°/90°/0°$ Cross-ply (50%-50%)	0.5	2.38
GLARE 6	2024-T3	0.2-0.5	$+45°/-45°$ Cross-ply (50%-50%)	0.25	2.52

Table 2 Mechanical properties of GLARE

Material	E_{11} (GPa)	E_{22} (GPa)	G_{12} (GPa)	v_{12}
2024- T3 Aluminum	72	72	26.6	0.33
Glass Fiber	86	86	32.3	0.33
Epoxy	3.4	3.4	1.26	0.35

3 ANALYTICAL PREDICTION BY MODIFIED LAMINATED PLATE THEORY

An analytical model incorporating the elasto-plastic behavior of aluminum sheets of GLARE is used to determine the stress-strain relation of GLARE. The most important assumptions for composite analysis assessed by Modified Laminated Plate theory are: composite fibers in the layers are parallel, distance between fibers in layers are equal, fibers are stretched along all layers and cross at some sections, and fibers are in perfect matrix bonding [19]. For a general orthotropic laminate subjected to in–plane loading, strain varies linearly in thickness direction but stress vary just linear in thickness direction in any layer. Therefore, an equivalent force–moment system replacing stress is used as following [19]:

$$\begin{Bmatrix} N \\ M \end{Bmatrix} = \begin{bmatrix} A & B \\ B & D \end{bmatrix} \begin{Bmatrix} \varepsilon^{\circ} \\ k \end{Bmatrix} \tag{1}$$

where A, B and D matrices are calculated as [19]:

$$[A, B, D] = \int_{-h/2}^{h/2} [Q](1, z, z^2) dz \tag{2}$$

GLARE 4- 3/2 and GLARE 5-2/1 are orthotropic and symmetrical with respect to the mid-plane. Thus, matrix B and $D_{16} = D_{26} = 0$ ($(2,6)$, $(1,6)$ elements of matrix D are zero). Therefore, the resultant forces and moments are obtained as:

$$[N, M] = \int_{-h/2}^{h/2} [\sigma]^i (1, z) dz \tag{3-a}$$

$$\begin{bmatrix} \sigma_{11} \\ \sigma_{22} \\ \sigma_{12} \end{bmatrix}^i = \begin{bmatrix} Q_{11} & Q_{12} & 0 \\ Q_{12} & Q_{22} & 0 \\ 0 & 0 & Q_{66} \end{bmatrix}^i \tag{3-b}$$

$$\left(\begin{bmatrix} \varepsilon_{11}^{\circ} \\ \varepsilon_{22}^{\circ} \\ \varepsilon_{12}^{\circ} \end{bmatrix} + z \begin{bmatrix} k_{11} \\ k_{22} \\ k_{12} \end{bmatrix} \right)^i$$

where $[\sigma]^i$ is the stress in i th ply at a distance z. Due to compatibility of the layers in GLARE laminate, all layers experience same deformation [20]. Under a uniaxial in-plane tensile load, the deformation response of the laminate is described by the following relation [20]:

$$dN = [A][d\varepsilon] \tag{4}$$

where dN can be expressed as:

$$dN = h[d\sigma] \tag{5}$$

The reduced stiffness matrix A is calculated as:

$$[A] = n_{AL} h_{AL} [Q]_{AL} + n_C h_C [Q]_C \tag{6}$$

3.1. Glass/epoxy Composite Model

The Glass/epoxy lamina is assumed to be a linear orthotropic elastic solid and the incremental stress- strain relation is [20]:

$$[d\sigma^C] = [Q]_C [d\varepsilon^C] \tag{7-a}$$

$$[d\sigma^C] = \{d\sigma^C_{11} \quad d\sigma^C_{22} \quad d\sigma^C_{12}\}^T \tag{7-b}$$

$$[d\varepsilon^C] = \{d\varepsilon^C_{11} \quad d\varepsilon^C_{22} \quad d\varepsilon^C_{12}\}^T \tag{7-c}$$

where $[Q]_C$ is:

$$[Q]_C = \begin{bmatrix} \dfrac{E_{11}}{L} & \dfrac{-v_{12}E_{22}}{L} & 0 \\ \dfrac{-v_{12}E_{22}}{L} & \dfrac{E_{22}}{L} & 0 \\ 0 & 0 & G_{12} \end{bmatrix}^C, \tag{8}$$

$$L = 1 - v_{12}{}^C v_{21}{}^C$$

3.2. Constitutive Model for 2024 – T3 Aluminum

In this study, the 2024- T3 aluminum is considered to be orthotropic elasto–plastic solid. Thus, it is necessary to divide 2024–T3 aluminum alloy into two models, which the first model denotes elastic deformation and the second model describes plastic deformation behavior. The elastic part of the aluminum deformation equation [20] is given by:

$$[d\varepsilon]_{EL} = [S_{AL}]_{EL} [d\sigma^{AL}]^{EL} \tag{9}$$

where $[S_{AL}]_{EL}$ is:

$$[S_{AL}]_{EL} = \begin{bmatrix} \dfrac{1}{E} & \dfrac{-v}{E} & 0 \\ \dfrac{-v}{E} & \dfrac{1}{E} & 0 \\ 0 & 0 & \dfrac{1}{G} \end{bmatrix}^{AL} \qquad (10)$$

For the plastic deformation of the aluminum, the plastic potential is defined as [20]:

$$f^{AL}(\sigma_{ij}) = \frac{1}{2}\left[a_{11}(\sigma_{11}^{AL})^2 + (\sigma_{22}^{AL})^2 - \sigma_{11}^{AL}\sigma_{22}^{AL} + 3(\sigma_{12}^{AL})^2\right] \qquad (11)$$

where a_{11} denotes the difference between the plastic portions of longitudinal and transverse directions. In this study, the power law is used to show the relationship between the effective stress and the effective plastic strain as defined below used as:

$$\bar{\varepsilon}_P^{AL} = \beta^{AL}(\bar{\sigma}^{AL})^\gamma \qquad (12)$$

Thus,

$$d\lambda_{AL} = \frac{3d\bar{\varepsilon}_P^{AL}}{2\bar{\sigma}^{AL}} = \Omega\left[\psi_1 d\sigma_{11}^{AL} + \psi_2 d\sigma_{22}^{AL} + \psi_3 d\sigma_{12}^{AL}\right] \qquad (13)$$

$$\Omega = \frac{9}{4}\beta_{AL}\gamma(\bar{\sigma}^{AL})^{\gamma-3} \qquad (14\text{-a})$$

$$\psi_1 = \frac{1}{2}\left(2a_{11}\sigma_{11}^{AL} - \sigma_{22}^{AL}\right) \qquad (14\text{-b})$$

$$\psi_2 = \frac{1}{2}\left(2\sigma_{22}^{AL} - \sigma_{11}^{AL}\right) \qquad (14\text{-c})$$

$$\psi_3 = 3\sigma_{12}^{AL} \qquad (14\text{-d})$$

The relation between plastic strain increment and the stress increment are presented as:

$$[d\varepsilon^{AL}]^P = [S_{AL}]_P[d\sigma^{AL}]^P \qquad (15)$$

where $[S_{AL}]_P$ is:

$$[S_{AL}]_P = \begin{bmatrix} \Omega\psi_1\psi_1 & \Omega\psi_1\psi_2 & \Omega\psi_1\psi_3 \\ \Omega\psi_1\psi_2 & \Omega\psi_2\psi_2 & \Omega\psi_2\psi_3 \\ \Omega\psi_1\psi_3 & \Omega\psi_2\psi_3 & \Omega\psi_3\psi_3 \end{bmatrix}_P^{AL} \qquad (16)$$

Therefore, the stress-strain relation for the aluminum is:

$$\begin{aligned} &[d\varepsilon^{AL}] = [S_{AL}][d\sigma^{AL}], \\ &[S_{AL}] = [S_{AL}]_{EL} + [S_{AL}]_P \\ &[d\sigma^{AL}] = [Q_{AL}][d\varepsilon^{AL}], \\ &[Q_{AL}] = [S_{AL}]^{-1} \end{aligned} \qquad (17)$$

4 AN ORTHOTROPIC PLASTICITY MODEL

The Second approach for achieving a nonlinear GLARE response is an orthotropic plasticity model. The case being analyzed is an, in plane plastic potential function with three parameters [21].

$$f(\sigma_{ij}) = \frac{1}{2}\left[a_{11}\sigma_{11}^2 + \sigma_{22}^2 + 2a_{12}\sigma_{11}\sigma_{22} + 2a_{66}\sigma_{12}^2\right] \qquad (18)$$

Note that Eq. (11) is a specialized case of Eq. (18) when $a_{66} = \dfrac{3}{2}$, $a_{12} = \dfrac{-1}{2}$. For elastic-plastic response of aluminum, the flow rule is used as follows:

$$d\varepsilon_{ij}^p = d\lambda\frac{\partial f}{\partial \sigma_{ij}} \qquad (19)$$

From Eqs. (18) and (19), plastic strain increment is presented in matrix form as mentioned below:

$$\begin{Bmatrix} d\varepsilon_{11}^p \\ d\varepsilon_{22}^p \\ d\varepsilon_{12}^p \end{Bmatrix} = \begin{bmatrix} a_{11} & a_{12} & 0 \\ a_{12} & 1 & 0 \\ 0 & 0 & 2a_{66} \end{bmatrix}\begin{Bmatrix} \sigma_{11} \\ \sigma_{22} \\ \sigma_{12} \end{Bmatrix}d\lambda \qquad (20)$$

where subscripts 1 and 2 indicate the fiber and transverse directions, respectively. The effective stress can be defined as [21]:

$$\bar{\sigma} = \sqrt{3f} \qquad (21)$$

also the effective plastic strain increment is defined as [21]:

$$d\bar{\varepsilon}^p = \left(\frac{2}{3(a_{11}-a_{12}^2)}\right)^{1/2} \qquad (22)$$

$$\left(\begin{array}{l}(d\varepsilon_{11}^p)^2 + a_{11}(d\varepsilon_{22}^p)^2 - 2a_{12}d\varepsilon_{11}^p d\varepsilon_{22}^p \\ + \dfrac{(a_{11}-a_{12}^2)}{2a_{66}}(d\varepsilon_{12}^p)^2\end{array}\right)^{1/2}$$

Thus, plastic work increment can be written as:

$$dW^p = \sigma_{ij} d\varepsilon_{ij}^p = \overline{\sigma} d\overline{\varepsilon}^p = 2fd\lambda \qquad (23)$$

Therefore, $d\lambda$ is derived as:

$$d\lambda = \frac{3d\overline{\varepsilon}^p}{2\overline{\sigma}} = \frac{3}{2}\left(\frac{d\overline{\varepsilon}^p}{d\overline{\sigma}}\right)\left(\frac{d\overline{\sigma}}{\overline{\sigma}}\right) \qquad (24)$$

To complete the stress-strain incremental plastic relation, the relation between the effective stress and effective plastic strain should be estimated. Thus, the power law should be used as [21]:

$$\overline{\varepsilon}^p = \beta(\overline{\sigma})^\gamma \qquad (25)$$

By considering the $x - y$ and $x_1 - y_1$ coordinates (see Fig. 1) and uniaxial stress in x direction and using rotational matrix T, the principle stresses are:

$$\begin{Bmatrix} \sigma_{11} \\ \sigma_{22} \\ \sigma_{12} \end{Bmatrix} = [T]\begin{Bmatrix} \sigma_x \\ 0 \\ 0 \end{Bmatrix} \qquad (26)$$

$$\sigma_{11} = \sigma_x \cos^2\theta$$
$$\sigma_{22} = \sigma_x \sin^2\theta$$
$$\sigma_{12} = -\sigma_x \sin\theta\cos\theta$$

Using the introduced rotational matrix for strains and Eqs. (18)-(22), gives:

$$\overline{\sigma} = g(\theta)\sigma_x \qquad d\overline{\varepsilon}^p = \frac{d\varepsilon_x^p}{g(\theta)} \qquad (27)$$

where ε_x^p denotes plastic strain in x direction and $g(\theta)$ is [21]:

$$g(\theta) = \sqrt{\frac{3}{2}}\left(a_{11}\cos^4\theta + \sin^4\theta + 2(a_{12}+a_{66})\sin^2\theta\cos^2\theta\right)^{1/2} \qquad (28)$$

Thus, the desired relation between $\overline{\varepsilon}^p - \overline{\sigma}$ can be obtained from the ε^p, σ_x and Eq. (28). Now, the single problem at hand is to assign values to a_{66}, a_{12}, a_{11}, in order to achieve the $\overline{\varepsilon}^p - \overline{\sigma}$ relation. Plastic Poisson's ratio definition is one way for selection of these parameters. Using Eqs. (20) and (26) and the coordinate transformation on strain components, the

plastic strain increments in the x and y directions can be obtained as:

$$d\varepsilon_x^p = d\lambda\sigma_x\begin{pmatrix} a_{11}\cos^4\theta + \sin^4\theta + \\ 2(a_{12}+a_{66})\sin^2\theta\cos^2\theta \end{pmatrix} \qquad (29\text{-}a)$$

$$d\varepsilon_y^p = d\lambda\sigma_x\begin{pmatrix} (1+a_{11}-2a_{66})\sin^2\theta\cos^2\theta + \\ a_{12}(\sin^4\theta + \cos^4\theta) \end{pmatrix} \qquad (29\text{-}b)$$

Thus, the plastic Poisson's ratio is:

$$v^p = -\frac{d\varepsilon_y^p}{d\varepsilon_x^p} = -\frac{(1+a_{11}-2a_{66})\sin^2\theta\cos^2\theta + a_{12}(\sin^4\theta+\cos^4\theta)}{a_{11}\cos^4\theta + \sin^4\theta + 2(a_{12}+a_{66})\sin^2\theta\cos^2\theta} \qquad (30)$$

Using above equations and Poisson's ratios in $\theta = 0°, 90°, 45°$, the plastic Poisson's ratios are:

$$v^p(\theta = 0) = -\frac{a_{12}}{a_{11}} \quad, \qquad (31)$$
$$v^p(\theta = 90) = -a_{12} \quad,$$
$$v^p(\theta = 45) = -\frac{1+a_{11}+2(a_{12}-a_{66})}{1+a_{11}+2(a_{12}+a_{66})}$$

Simplifying Eqs.(31) gives:

$$\qquad (32)$$
$$a_{11} = \frac{v^p(\theta = 90)}{v^p(\theta = 0)}$$
$$a_{12} = -v^p(\theta = 90)$$
$$a_{66} = -\frac{1 + \left[v^p(\theta=90)\middle/v^p(\theta=0)\right] - 2v^p(\theta=90)}{2} = $$
$$-\frac{1 + a_{11} + 2a_{12}}{2}$$

5   RESULTS AND DISCUSSION

In order to illustrate the behavior of the GLARE 4-3/2 and GLARE 5-2/1 under longitudinal and transverse loading conditions, the following table is presented.

Table 3 Geometrical properties of the GLARE

Material	Thickness (mm)	Length (mm)	Width (mm)
Aluminum 2024-T3	0.489	305	25.5
Glass/epoxy Composite	0.548	305	25.5

5.1. Inelastic behavior of GLARE by Modified Laminated Plate Model

To use the laminated plate model, it is necessary to assign values $a_{11}, \gamma, \beta_{AL}$. Thus, for fiber orientation $\theta = 0°, 90°$ can be written, $g(90) = \sqrt{\frac{3}{2}}$, $g(0) = \sqrt{\frac{3}{2}} a_{11}$ where effective stress and effective plastic strain relations are independent of parameter a_{11} in $\theta = 90°$. This can be noted to calculate parameters γ, β_{AL}. By using the least square method, we have $\beta_{AL} = 0.478 \times 10^4$, $\gamma = 15$, and $a_{11} = 0.787$ under uniaxial loading condition; the stress-strain curve is shown in Fig. 2.
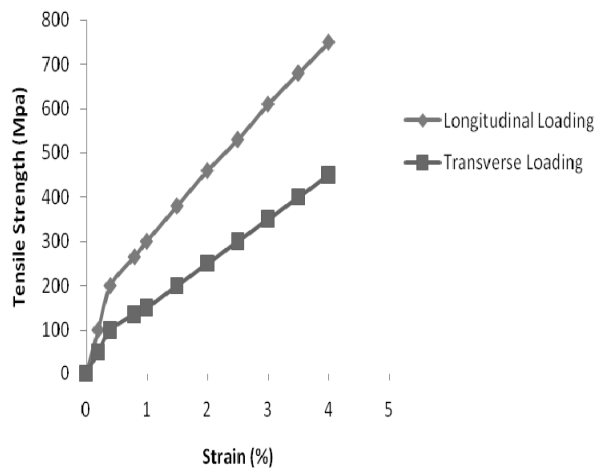
Fig. 2 Stress-strain curve of GLARE 4-3/2 in longitudinal and transverse loading acquired from modified laminated plate model
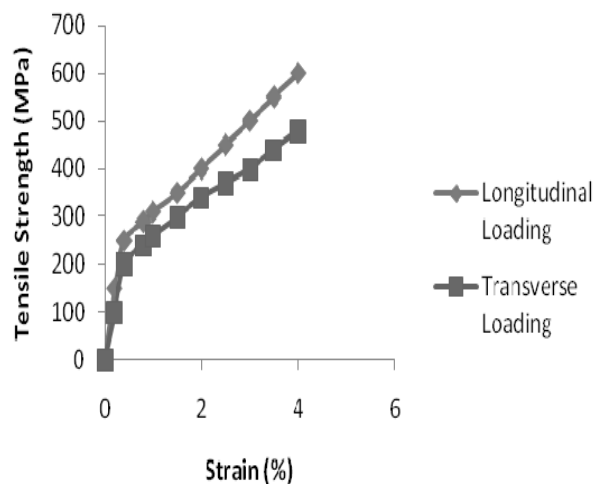
Fig. 3 Stress-strain curve of GLARE 5-2/1 in longitudinal and transverse loading from modified laminated plate model

The tensile response of GLARE 4-3/2 and GLARE 5-2/1 are presented in figures 2 and 3. As depicted in the mentioned figures, it can be concluded that both GLAREs' behavior vary almost linearly in plastic part similar to elastic region in the longitudinal loading. In the transverse loading, a similar stress-strain response to the longitudinal direction is obtained. This explains that GLARE 4-3/2 and GLARE 5-2/1 exhibit a bilinear stress-strain behavior in the both longitudinal and transverse directions. Results show that the stress–strain relation of GLARE 5-2/1 is similar to that of GLARE 4-3/2. However, GLARE 5-2/1 exhibits the same modulus in both the longitudinal and transverse directions due to the 0°/90°/90°/0° Glass/epoxy layers. Of course, the stress-strain response specifications such as yield stress, hardening modulus and tensile fracture stress in the transverse loading are lower than longitudinal direction due to 0°/90°/90°/0° orientation of fibers. It can be seen that both GLAREs has two different slopes in elastic and plastic parts. It means that elastic modulus and hardening modulus are not equal. Fig. 4 shows the Poisson's ratio response of GLARE 4 and GLARE 5 for the longitudinal direction. It can be seen that Poisson's ratio response for GLARE 5-2/1 is lower than the similar case in longitudinal loading of GLARE 4-3/2. This fact is due to $0°/90°/90°/0°$ fibers orientation as described above.
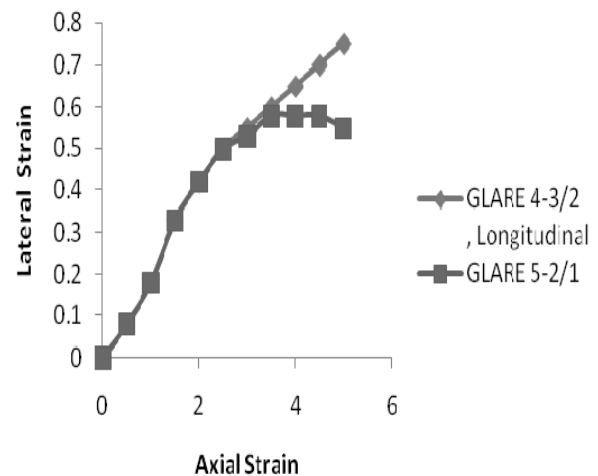
Fig. 4 The Poisson's ratio response in longitudinal direction for GLARE 4, 5

5.2. Elasto–plastic deformation of GLARE via Orthotropic Plasticity Model

By considering the orthotropic plasticity model for the GLARE laminate, all longitudinal stress-strain curves should be replaced by a single curve indicating effective stress and effective plastic strain. This is the basis for determining the values of a_{11}, a_{12} and a_{66} in the plastic potential function. From Eq. (28) it can be

concluded that $g(90) = \sqrt{\dfrac{3}{2}}$ and is independent of a_{11}, a_{12} and a_{66} parameters. Using the stress- strain curve of the $\theta = 90^0$, $\beta = 55.2$ and $\gamma = 8.05$ for values of parameters a_{11} and $a_{12} + a_{66}$ in $g(\theta)$ should make the effective stress and effective plastic strain curves fall on the stress-strain curve for $\theta = 90^0$. Thus, a reasonable set of values for the introduced parameters would be: $a_{11} = 0.36$ and $a_{12} + a_{66} = 1.3$. The tensile stress-strain relation for GLARE 4-3/2 and GLARE 5-2/1 in both the longitudinal and transverse directions has been shown in figures 5 and 6.
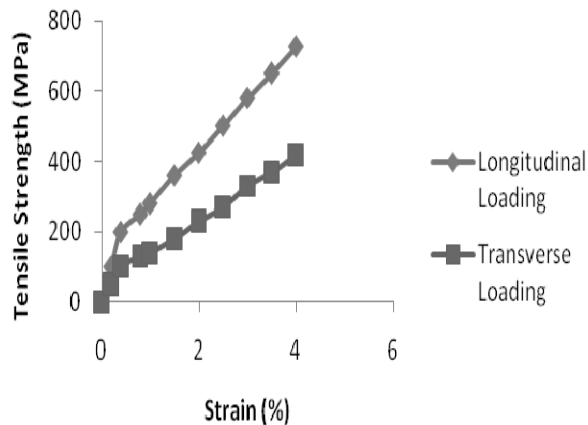
Fig. 5   Stress-strain curve of GLARE 4-3/2 in longitudinal and transverse loading from orthotropic plasticity mode
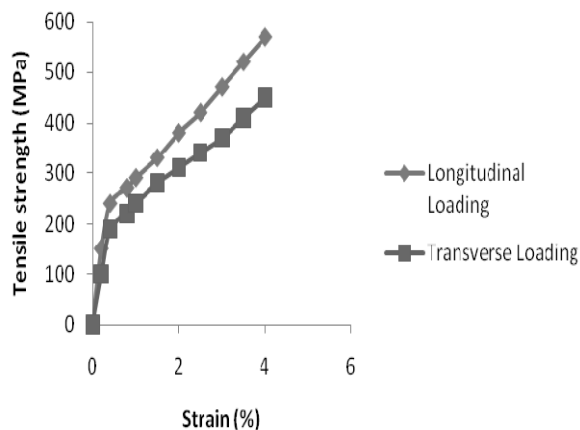
Fig. 6   Stress-strain curve of GLARE 5-2/1 in longitudinal and transverse loading from orthotropic plasticity model

6   CONCLUSIONS

In this paper the nonlinear behavior of GLARE 4-3/2 and GLARE 5-2/1 under in–plane tensile loading has been investigated. Two approaches namely orthotropic plasticity and modified laminated plate theories were used to predict the elastic-plastic behavior of GLARE laminates. In the modified laminated plate approach, aluminum layers in GLAREs have been modeled as orthotropic elasto-plastic solids and Glass/epoxy layers have been considered as orthotropic linearly elastic solids. Results showed that GLAREs are stronger than aluminum alloy and stress-strain relations are almost bilinear in both longitudinal and transverse directions. The stress-strain response indicates that both GLAREs have more strength in longitudinal direction in comparison to transverse direction. Analytical predictions by modified laminated plate theory showed good agreement with results of orthotropic plasticity model. It has been seen that Poisson's ratio response in GLARE 5 is lower than the similar case in longitudinal loading of GLARE 4 due to $0°/90°/90°/0°$ orientation of fibers.

7   NOMENCLATURE

N	In – plane force per unit length
M	In – plane moment per unit length
$\varepsilon°$	The mid-plane strains
k	The mid-plane curvature
A	Extensional stiffness matrix
B	Coupling stiffness matrix
D	Bending stiffness matrix
h	Laminate thickness
$[Q]$	Reduced stiffness matrix
$[Q]_c$	Glass/epoxy composite stiffness matrix
$f(\sigma_{ij})$	Plastic potential function
dN	Increments of the in - plane force per unit length
$h_{AL/c}$	Thickness aluminum/ composite layers

$n_{AL/c}$	Number of aluminum/ composite layers
$[S_{AL}]_{EL/P}$	Aluminum alloy flexibility matrix for elastic/plastic deformation
$d\lambda$	Proportional factor.
E	Elastic modulus
ν	Poisson's ratio
G	Shear modulus
T	Rotational matrix
$d\varepsilon_{ij}^{p}$	Plastic strain increment
$\bar{\varepsilon}^{p}$	Effective plastic strain
$\bar{\sigma}$	Effective stress

REFERENCES

[1] Vermeeren, C. A. J. R., "An Historic Overview of the Development of Fiber Metal Laminates, Applied Composite Materials", Vol. 10, No. 4-5, 2003, pp. 189-205.

[2] Gay, D., "Composite Materials Design and Application", CRC Press, 2003.

[3] Vinson, J. R. and Seirakowski, R. L., "The Behavior of Structures Composed of Composite Materials", 2nd Edition, Springer, 2004.

[4] Soutis, C., "Fiber Reinforced Composites in Aircraft Construction, Progress in Aerospace Sciences", Vol. 41, No. 2, 2005, pp. 143-151.

[5] Vlot, A., Vogelesang, L. B., De Vries, T. J., "Towards Application of Fiber Metal Laminates in Large Aircraft", Aircraft Engineering and Aerospace Technology, Vol. 71, No. 6, 1999, pp. 558-570.

[6] Vogelesang, L. B., Vlot, A., "Development o f Fiber Metal Laminates for Advanced Aerospace Structures", Material Processes Technology, Vol. 103, 2000, pp. 1-5.

[7] Gunnink, J. W., Vlot, A., Deveries T. J., Hoeven, W. V., GLARE Technology Development, Applied Composite Materials", Vol. 9, No. 4, 2002, pp. 201-219.

[8] Frizzel, R. M., McCarthy, C. T., McCarthy, M. A., "A Comparative Study of the Pin-Bearing Responses of Two Glass-Based Fiber Metal Laminates", Composites Science and Technology, Vol. 68, 2008, pp. 3314-3321.

[9] Wu, G., Yang, J. M., "The Mechanical Behavior of GLARE Laminates for Aircraft Structures", JOM Journal of the Minerals, Metals and Materials Society, Vol. 57, No. 1, 2005, pp. 72-79.

[10] Botelho, E. C., Silva, R. A., Pardini, L. C., Rezende, M. C., A Review on the Development and Properties of Continuous Fiber/Epoxy/Aluminum Hybrid Composites for Aircraft Structures, Materials Research, Vol. 9, No. 3, 2006, pp. 247-256.

[11] Sadighi, M., Dariushi, S., "An Experimental Study of the Fiber Orientation and Laminate Sequencing Effects on Mechanical Properties of GLARE", Proceedings of the Institution of Mechanical Engineers, Part G: Journal of Aerospace Engineering, Vol. 222, No. 7, 2008, pp. 1015-1024.

[12] Sinke, J., "Development of Fiber Metal Laminates: Concurrent Multi-Scale Modeling and Testing", Journal of Materials Science, Vol. 41, No. 20, 2006, pp.6777-6788.

[13] Chen, J. L., Sun, C. T., "Modeling of Orthotropic Elastic–Plastic Properties of ARALL Laminates, Composites Science and Technology", Vol. 36, No. 4, 1989, pp.321-337.

[14] Wu, G., Yang, J. M., Analytical Modelling and Numerical Simulation of the Nonlinear Deformation o f Hybrid Fiber–Metal Laminates, Modelling and Simulation in Materials Science and Engineering, Vol. 13, No. 3, 2005, pp. 413-425.

[15] Krishnakumar, S., Fiber Metal laminates-the Synthesis of Metals and Composites, Material and Manufacturing Processes, Vol. 9, 1994, pp. 295-354.

[16] Vlot, A., Kroon, E., Rocca, G., Impact Response of Fiber Metal Laminates, Key Engineering Material, Vol.141-143, 1998, pp.235-76.

[17] Wu, H. F., Wu, L. L., Use of Rule of Mixtures and Metal Volume Fraction for Mechanical Property Predictions of Fiber-Reinforced Aluminum Laminates, Journal of Materials Science, Vol. 29, No. 17, 1994, pp. 4583-4591.

[18] Nahas, M. N., Analysis of Non-Linear Stress-Strain Response of Laminated Fiber-Reinforced Composites, Fiber Science and Technology, Vol. 20, No. 4, 1984, pp. 297-313.

[19] Jones, R. M., Mechanics o f Composite Materials, 2nd Edition, Philadelphia, Taylor and Francis, 1998.

[20] Herakovich, C. T., Mechanical and Thermal Characterization of Unidirectional Aramid/Epoxy, Presented at ARALL Laminates Technical Conference, Pennsylvania, USA, 1987, pp. 25-8.

[21] Kenaga, D., Doyle, J. F., Sun, C. T., The Characterization of Boron/Aluminum Composite in Nonlinear Range as an Orthotropic Elastic- Plastic Material, Journal of Composite Material, Vol. 21, No. 6, 1987, pp. 516-531.